

## PROMPT OPTICAL DETECTION OF GRB 050401 WITH ROTSE-IIIa

RYKOFF, E. S.<sup>1</sup>, YOST, S. A.<sup>1</sup>, KRIMM, H. A.<sup>2,3</sup>, AHARONIAN, F.<sup>4</sup>, AKERLOF, C. W.<sup>1</sup>, ALATALO, K.<sup>1</sup>, ASHLEY, M. C. B.<sup>5</sup>, BARTHELMY, S. D.<sup>2</sup>, GEHRELS, N.<sup>2</sup>, GÜVER, T.<sup>6</sup>, HORNS, D.<sup>4</sup>, KIZILOĞLU, Ü.<sup>7</sup>, MCKAY, T. A.<sup>1</sup>, ÖZEL, M.<sup>8</sup>, PHILLIPS, A.<sup>5</sup>, QUIMBY, R. M.<sup>9</sup>, RUJOPAKARN, W.<sup>1</sup>, SCHAEFER, B. E.<sup>10</sup>, SMITH, D. A.<sup>1</sup>, SWAN, H. F.<sup>1</sup>, VESTRAND, W. T.<sup>11</sup>, WHEELER, J. C.<sup>9</sup>, WREN, J.<sup>11</sup>

*Draft version February 5, 2008*

### ABSTRACT

The ROTSE-IIIa telescope at Siding Spring Observatory, Australia, detected prompt optical emission from *Swift* GRB 050401. In this letter, we present observations of the early optical afterglow, first detected by the ROTSE-IIIa telescope 33 s after the start of  $\gamma$ -ray emission, contemporaneous with the brightest peak of this emission. This GRB was neither exceptionally long nor bright. This is the first prompt optical detection of a GRB of typical duration and luminosity. We find that the early afterglow decay does not deviate significantly from the power-law decay observable at later times, and is uncorrelated with the prompt  $\gamma$ -ray emission. We compare this detection with the other two GRBs with prompt observations, GRB 990123 and GRB 041219a. All three bursts exhibit quite different behavior at early times.

*Subject headings:* gamma rays:bursts

### 1. INTRODUCTION

The detection of prompt optical emission contemporaneous with gamma-ray bursts (GRBs) has been quite difficult. Until now, only two bursts, GRB 990123 and GRB 041219a, have had optical light detected while detectable  $\gamma$ -rays were still being emitted. The ROTSE-I instrument detected a bright 9<sup>th</sup> magnitude flash coincident with GRB 990123, a burst exceptionally luminous in  $\gamma$ -rays (Akerlof et al. 1999). The RAPTOR-S telescope detected faint optical emission from GRB 041219a that was correlated with the  $\gamma$ -ray emission (Vestrand et al. 2005, henceforth, V05). GRB 041219a was an unusually long burst (over 6 minutes) that allowed extended optical monitoring during the  $\gamma$ -ray emission. The *Swift* detection of GRB 050401 and rapid dissemination of

its coordinates enabled the first prompt detection of an optical counterpart for a GRB with a typical duration and fluence. With a T90 of 33 s and a fluence of  $1.4 \times 10^{-5}$  erg cm<sup>-2</sup> in the 15-350 keV band (Sakamoto et al. 2005), this burst was neither especially long nor bright.

In this letter, we report on the prompt detection of the optical afterglow of GRB 050401 with the ROTSE-IIIa (Robotic Optical Transient Search Experiment) telescope located at Siding Spring Observatory (SSO), Australia. Our initial detection of the afterglow is coincident with the brightest peak in the  $\gamma$ -ray emission. ROTSE-IIIa followed the afterglow through the first four minutes after the burst, recording a fading afterglow consistent with a backward extrapolation of the afterglow measured at much later times. We compare these observations to the two previously observed cases of prompt optical emission, and to the empirical model of V05 that suggested a coupling of  $\gamma$ -ray and optical flux.

### 2. OBSERVATIONS AND ANALYSIS

The ROTSE-III array is a worldwide network of 0.45 m robotic, automated telescopes, built for fast ( $\sim 6$  s) responses to GRB triggers from satellites such as HETE-2 and *Swift*. They have wide ( $1.85 \times 1.85$ ) fields of view imaged onto Marconi 2048  $\times$  2048 back-illuminated thinned CCDs, and operate without filters. The ROTSE-III systems are described in detail in Akerlof et al. (2003).

On 2005 April 01, *Swift*/BAT detected GRB 050401 (*Swift* trigger 113120) at 14:20:15 UT. The position was distributed as a Gamma-ray Burst Coordinates Network (GCN) notice at 14:20:34 UT, with a 4' radius error box. The burst had a T<sub>90</sub> duration of  $33 \pm 2$  s, and the position was released during the  $\gamma$ -ray emission (Sakamoto et al. 2005). The *Swift* trigger time was 9 seconds after the start of the GRB; in this paper we reference all times to the start of  $\gamma$ -ray emission at 14:20:06 UT.

ROTSE-IIIa responded automatically to the GCN notice, beginning its first exposure in less than 6 seconds, at 14:20:39.2 UT, during the largest peak of the  $\gamma$ -ray emission. The automated burst response included a set of ten

<sup>1</sup> University of Michigan, 2477 Randall Laboratory, 450 Church St., Ann Arbor, MI, 48109, erykoff@umich.edu, sayost@umich.edu, akerlof@umich.edu, kalatalo@umich.edu, tamckay@umich.edu, wiphu@umich.edu, donaldas@umich.edu, hswan@umich.edu

<sup>2</sup> NASA Goddard Space Flight Center, Laboratory for High Energy Astrophysics, Greenbelt, MD 20771, krimm@milkyway.gsfc.nasa.gov, scott@milkyway.gsfc.nasa.gov, gehrels@milkyway.gsfc.nasa.gov

<sup>3</sup> Universities Space Research Association, 10227 Wincopin Circle, Suite 212, Columbia, MD 21044

<sup>4</sup> Max-Planck-Institut für Kernphysik, Saupfercheckweg 1, 69117 Heidelberg, Germany, Felix.Aharonian@mpi-hd.mpg.de, horns@mpi-hd.mpg.de

<sup>5</sup> School of Physics, Department of Astrophysics and Optics, University of New South Wales, Sydney, NSW 2052, Australia, mcba@phys.unsw.edu.au, a.phillips@unsw.edu.au

<sup>6</sup> Istanbul University Science Faculty, Department of Astronomy and Space Sciences, 34119, University-Istanbul, Turkey, tolga@istanbul.edu.tr

<sup>7</sup> Middle East Technical University, 06531 Ankara, Turkey, umk@astroa.physics.metu.edu.tr

<sup>8</sup> Çanakkale Onsekiz Mart Üniversitesi, Terzioglu 17020, Çanakkale, Turkey, m.e.ozel@comu.edu.tr

<sup>9</sup> Department of Astronomy, University of Texas, Austin, TX 78712, quimby@astro.as.utexas.edu, wheel@astro.as.utexas.edu

<sup>10</sup> Department of Physics and Astronomy, Louisiana State University, Baton Rouge, LA 70803, schaefer@lsu.edu

<sup>11</sup> Los Alamos National Laboratory, NIS-2 MS D436, Los Alamos, NM 87545, vestrand@lanl.gov, jwren@nis.lanl.gov

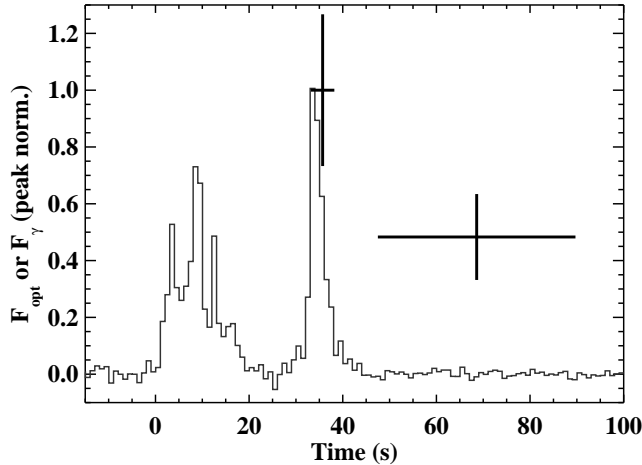


FIG. 1.—  $\gamma$ -ray lightcurve for GRB 050401. The time is seconds since the start of  $\gamma$ -ray emission at 14:20:06 UT. The burst T90 duration was  $33 \pm 2$  s. The first two optical detections (peak normalized) have been overplotted. The first ROTSE-IIIa observation is coincident with the brightest  $\gamma$ -ray peak, and there is no correlation between the  $\gamma$ -ray flux and the optical flux at the early time.

5-s exposures, ten 20-s exposures, and a long sequence of 60-s exposures continuing for about 5 hours until twilight. Initial analysis of the prompt response did not yield an obvious afterglow candidate. About an hour after the burst, at 15:17:16.8 UT, McNaught & Price (2005) initiated a burst response on the SSO 40-inch telescope. They detected a new 20<sup>th</sup> magnitude object at  $\alpha = 16^h 31^m 28^s.8$ ,  $\delta = 02^\circ 11' 14''$  (J2000.0) which they identified as the optical counterpart. Further analysis of the ROTSE-IIIa images revealed this source at magnitudes close to our detection limit. Later spectroscopic observations by Fynbo et al. (2005) at the VLT revealed a redshift of 2.9 for this burst. The burst position has a high galactic latitude of 31.8°, so extinction from the Milky Way is not significant.

The  $\gamma$ -ray light curve from the *Swift*/BAT instrument is shown in Figure 1. The light curve has been normalized to the peak flux. Overplotted are the first two ROTSE-IIIa observations, with the first 5-s integration coincident with the brightest peak in the  $\gamma$ -ray emission. That burst was 56 degrees from the spacecraft axis, which means that the source illuminated only 8% of the BAT detectors (Barthelmy et al. 2005). The *Swift* spacecraft began its slew to the target during the ROTSE-IIIa observation, delayed by 9 seconds due to an earth-limb constraint. All the BAT flux values were corrected for partial illumination and other geometric effects, including the spacecraft slew. The  $\gamma$ -ray spectrum during this period is well fit by a simple power law with a photon index of  $1.58 \pm 0.06$ , with a  $\chi^2$  of 58.0 (57 d.o.f.). This is consistent with the index early in the burst suggesting that there is no significant spectral evolution. Table 1 shows the flux density and flux measurements for the  $\gamma$ -ray emission coincident with the first two ROTSE-IIIa observations. To obtain a  $3\sigma$  upper limit for the  $\gamma$ -ray flux coincident with the second ROTSE-IIIa integration, we assumed the source had the same spectral shape as the first integration.

The ROTSE-IIIa images were bias-subtracted and flat-fielded. The flat-field image was generated from 30 twi-

TABLE 1. SIMULTANEOUS ROTSE-III AND *Swift* MEASUREMENT OF GRB 050401.

Obs.	Energy Band	Flux Density (mJy)	Flux ( $\text{erg cm}^{-2} \text{s}^{-1}$ )
1	$R_c$ -band <sup>a</sup>	$0.59 \pm 0.16$	$6.6 \pm 1.8 \times 10^{-13}$
	15-350 keV	$7.60 \pm 24 \times 10^{-7}$	
	15-25 keV	$2.73 \pm 0.09$	$6.60 \pm 0.21 \times 10^{-8}$
	25-50 keV	$1.91 \pm 0.06$	$1.16 \pm 0.04 \times 10^{-7}$
	50-100 keV	$1.28 \pm 0.12$	$1.55 \pm 0.14 \times 10^{-7}$
	100-350 keV	$0.70 \pm 0.02$	$4.24 \pm 0.14 \times 10^{-7}$
2	$R_c$ -band <sup>a</sup>	$0.28 \pm 0.08$	$3.2 \pm 0.9 \times 10^{-13}$
	15-350 keV		$< 4.02 \times 10^{-8}$

NOTE. — Observation 1 is 33.2 s - 38.2 s post-burst, and observation 2 is 47.5 s - 89.7 s post-burst.

<sup>a</sup>The unfiltered ROTSE magnitudes have been calibrated such that they are roughly equivalent to the  $R_c$  band system.

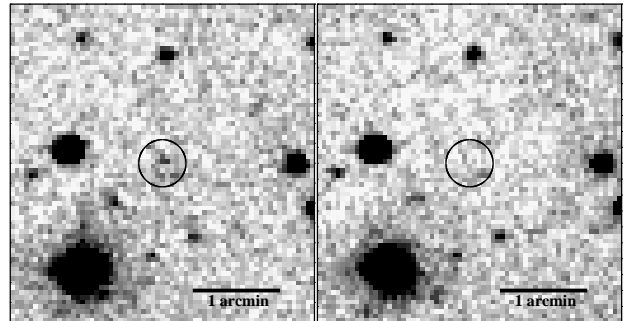


FIG. 2.— Optical counterpart of GRB 050401. The panel on the left shows the counterpart in a co-added image from 33 s to 281 s post-burst. The counterpart is absent from the panel on the right, a co-added image from 290 s to 487 s post-burst.

light images. We used SExtractor (Bertin & Arnouts 1996) to perform the initial object detection and to determine the centroid positions of the stars. After the first 5-s integration, images were co-added in sets of three to improve our signal to noise. The transient is not detected in individual frames, which have limits consistent with the magnitudes derived from the co-added frames. The images were then processed with a customized version of the DAOPHOT PSF fitting package (Stetson 1987) that has been ported to the IDL Astronomy User's Library (Landsman 1995). The magnitude zero-point for each image is calculated from the median offset to the USNO 1-m  $R$ -band standard stars (Henden 2005) in the magnitude range of  $13.5 < V < 20.0$  with  $0.4 < V - R < 1.0$ . As we have no data on afterglow color information at the early time, no additional color corrections have been applied to our unfiltered data.

Figure 2 shows the optical counterpart and a later non-detection image. The panel on the left is a co-addition of all our images with significant flux, from 33 s to 281 s post-burst. The panel on the right is the subsequent non-detection image from 290 s to 487 s post-burst. Table 2 contains the optical photometry for the early afterglow. In addition, Table 1 shows the approximate flux density for our first two observations, assuming the ROTSE-IIIa unfiltered magnitudes are roughly equivalent to the  $R_c$ -band system.

### 3. RESULTS

TABLE 2. OPTICAL PHOTOMETRY FOR GRB 050401

Telescope	Filter	$t_{\text{start}}$ (s)	$t_{\text{end}}$ (s)	Magnitude
ROTSE-IIIa	None	33.2	38.2	$16.80 \pm 0.29$
ROTSE-IIIa	...	47.5	89.7	$17.59 \pm 0.34$
ROTSE-IIIa	...	99.2	140.9	$17.42 \pm 0.23$
ROTSE-IIIa	...	150.2	184.3	$17.88 \pm 0.25$
ROTSE-IIIa	...	201.5	281.2	$18.58 \pm 0.43$
ROTSE-IIIa	...	290.3	487.1	$> 18.60$

NOTE. — All times are in seconds since the burst time, 14:20:06 UT (see § 2)

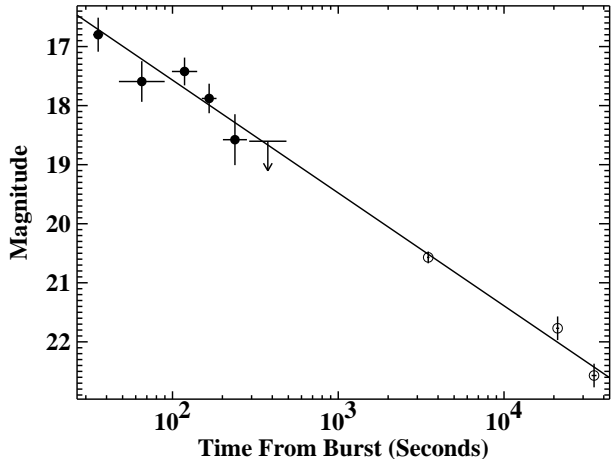


FIG. 3.— Optical lightcurve for GRB 050401. The filled circles are from ROTSE-IIIa and the empty circles are taken from the literature (Price & McNaught 2005; Kahharov et al. 2005; Misra et al. 2005). A power-law fit with a decay slope of  $\alpha = -0.76 \pm 0.03$  is overplotted. The early optical afterglow, including the first point coincident with the  $\gamma$ -ray emission, does not show any significant deviation from the power-law decay visible at later times.

Figure 3 shows the optical light curve of GRB 050401 with the ROTSE-IIIa observations combined with later followup from larger telescopes. The light curve for the first 40000 s is well fit by a single power-law  $f_\nu \propto t^\alpha$  with a decay slope  $\alpha = -0.76 \pm 0.03$  ( $\chi^2 = 4.7$ , 6 d.o.f.). Interestingly, there is no evidence that the afterglow is either brighter or dimmer during the prompt  $\gamma$ -ray emission than one would predict from an extrapolation of the later afterglow. We see no evidence for excess emission expected from a reverse shock flash, nor do we see evidence for a deficit of emission during the rise of the early afterglow.

With the detection of a prompt optical counterpart, we can compare the optical to  $\gamma$ -ray flux ratio from GRB 050401 to that of GRB 041219a and GRB 990123, the other two bursts with prompt detections. Following the method of V05, we have calculated the optical to  $\gamma$ -ray flux ratio  $F_{R_c}/F_\gamma$  for the prompt optical observation and the first subsequent co-added integration. As with V05, we use the flux integrated in the *Swift*/BAT 15–350 keV band over the duration of our observation. We have not performed any  $k$ -corrections because we do not know the spectral shape of the prompt optical emission.

The flux ratio for the first ROTSE-IIIa observation of GRB 050401 is  $8.7 \pm 2.3 \times 10^{-7}$ . We have tested the cor-

relation between the optical and  $\gamma$ -ray fluxes for the first two integrations. We fit a simple proportional model of the form  $F_{\text{opt}} = aF_\gamma$  using the two optical detections and the  $\gamma$ -ray detection and upper limit. This proportional model results in a very poor fit, with a  $\chi^2$  probability of 0.04%. Therefore, the  $\gamma$ -ray and optical flux are not correlated.

The flux ratio during the first ROTSE-III integration is  $\sim 14$  times dimmer in optical than that calculated for GRB 041219a in V05. If the flux ratio for GRB 050401 were the same as that for GRB 041219a, we would expect an optical detection at  $\sim 14$  magnitude. If the transient had been this bright we would have detected it with a S/N of over 25, which we can firmly rule out. In addition, V05 had to perform an approximate galactic reddening correction of 4.9 magnitudes, and suggest that the true extinction value may be larger. This would imply that the optical to  $\gamma$ -ray flux is even larger for GRB 041219a, and V05 would predict a brighter counterpart for GRB 050401.

We have also compared the prompt optical flux from GRB 050401 to that from GRB 990123. Although the optical emission from GRB 990123 is not correlated with the  $\gamma$ -ray emission, V05 have suggested that the first detection of the transient at 11<sup>th</sup> magnitude might be related to the brightest  $\gamma$ -ray peak. Using the GRB (“Band”) model parameters from Briggs et al. (1999), we have calculated the flux in the 15–350 keV band for the first ROTSE-I integration of GRB 990123. We find that the optical-to- $\gamma$ -ray flux ratio is  $1.7 \times 10^{-5}$ , or about a factor of 20 larger than that for GRB 050401. However, it is reasonable to expect that this first optical detection of GRB 990123 is the onset of the reverse shock, which is not evident in the early afterglow of GRB 050401.

The primary difficulty in comparing the optical flux to the  $\gamma$ -ray flux is that all three bursts have different spectral shapes in the  $\gamma$ -ray regime. Comparing the optical and  $\gamma$ -ray flux densities avoids the integration over the arbitrary  $\gamma$ -ray passband and can simplify the comparison of these different bursts. Table 3 shows the flux density at 1.9 eV (the peak of the  $R_c$  passband), 20 keV, and 100 keV for the three bursts. We have chosen to examine the first optical integration of GRB 990123, which might be before the onset of the reverse shock; the third optical integration of GRB 041219a, which is coincident with the final peak in the  $\gamma$ -ray emission; and the first optical integration of GRB 050401, also coincident with the final  $\gamma$ -ray peak. There does not seem to be any obvious pattern common to all three bursts.

#### 4. DISCUSSION

Although V05 have seen evidence for correlation between the optical flux and  $\gamma$ -ray flux for GRB 041219a, this correlation is absent in GRB 050401. Each of the three GRBs with prompt optical detections displays a different relationship between optical and  $\gamma$ -ray flux. For GRB 990123, the optical and  $\gamma$ -ray emission vary independently, and the optical emission is much brighter than a back extrapolation of the afterglow would suggest. For GRB 041219a, the optical and  $\gamma$ -ray emission are correlated, but we do not have any further observations to compare this to the later afterglow. Finally, for GRB 050401, the optical and  $\gamma$ -ray emission vary independently, and the prompt optical emission is well fit by

TABLE 3. FLUX DENSITIES FOR PROMPT COUNTERPARTS.

Burst	$F_{\text{opt}}$ (erg cm $^{-2}$ s $^{-1}$ )	$f_{\nu}$ [1.9 eV] (mJy)	$f_{\nu}$ [20 keV] (mJy)	$f_{\nu}$ [100 keV] (mJy)
GRB 990123 (1)	$1.0 \pm 0.1 \times 10^{-10}$	$89 \pm 12$	$3.4 \pm 0.3$	$5.7 \pm 0.3$
GRB 041219a (3)	$4.3 \pm 0.9 \times 10^{-12}$	$3.8 \pm 0.8$	$2.88 \pm 0.07$	$0.83 \pm 0.04$
GRB 050401	$6.6 \pm 1.8 \times 10^{-13}$	$0.59 \pm 0.16$	$2.73 \pm 0.09$	$0.99 \pm 0.12$

a backward extrapolation of the later afterglow emission.

As the prompt optical emission of GRB 050401 is indistinguishable from the later afterglow, it is most likely radiated from the same emitting region. In the fireball model (Piran 2005), the afterglow radiation is from the forward external shock. This would indicate that any optical emission related to the prompt  $\gamma$ -ray emission radiated by the internal shocks is negligible compared to the forward shock emission. As the optical observations began only 33 s after the start of the  $\gamma$ -ray emission, this would imply a very rapid rise in the forward shock emission. Therefore, the typical synchrotron peak,  $\nu_m$ , must have passed the optical band at  $< 30$  s. This is consistent with both an ISM environment (Sari & Esin 2001) and a wind environment (Chevalier & Li 2000) with small but reasonable values for the microphysical parameters. In addition, the lack of a reverse shock signature is consistent with a high density wind medium (Nakar & Piran 2004). This early behavior is quite different from the behavior of GRB 990123, GRB 041219a, and for other early afterglows such as that from GRB 030418 (Rykoff et al. 2004) that have been observed to rise after tens or hundreds of seconds.

The rapid localization of GRB 050401 by *Swift*, combined with the rapid response of the ROTSE-III instruments, has allowed, for the first time, the detection of a prompt optical counterpart of a typical GRB. *Swift* will localize  $\sim 75$  bursts per year, and the ROTSE-III instruments can promptly respond to  $\sim 40\%$  of these bursts. Many of these localizations will be during the  $\gamma$ -ray emission, and we expect the ROTSE-III instruments to achieve  $\sim 5$  prompt detections per year. During the next few years we will sample the range of prompt optical emission from GRBs, perhaps revealing patterns which will inform our understanding of the underlying GRB engine.

This work has been supported by NASA grants NNG-04WC41G and NNG-04WC41G, NSF grants AST-0407061, the Australian Research Council, the University of New South Wales, and the University of Michigan. Work performed at LANL is supported through internal LDRD funding. Special thanks to the observatory staff at Siding Spring Observatory.

#### REFERENCES

Akerlof, C., et al. 1999, *Nature*, 398, 400  
 Akerlof, C. W., et al. Jan. 2003, *PASP*, 115, 132  
 Barthelmy, S. D., et al. July 2005, To be published in *Space Science Reviews*, arXiv:astro-ph/0507410  
 Bertin, E. & Arnouts, S. June 1996, *A&AS*, 117, 393  
 Briggs, M. S., et al. Oct. 1999, *ApJ*, 524, 82  
 Chevalier, R. A. & Li, Z. June 2000, *ApJ*, 536, 195  
 Fynbo, J. P., et al. 2005, *GCN Circ.* No. 3176  
 Henden, A. 2005, *GCN Circ.* No. 3454  
 Kahharov, B., Ibrahimov, M., Sharapov, D., Pozanenko, A., Rumyantsev, V., & Beskin, G. 2005, *GCN Circ.* No. 3174  
 Landsman, W. B. 1995, , in *ASP Conf. Ser.* 77: *Astronomical Data Analysis Software and Systems IV*  
 McNaught, R. & Price, P. A. 2005, *GCN Circ.* No. 3163  
 Misra, K., Kamble, A. P., & Pandey, S. B. 2005, *GCN Circ.* No. 3175  
 Nakar, E. & Piran, T. Sept. 2004, *MNRAS*, 353, 647  
 Piran, T. 2005, *Reviews of Modern Physics*, 76, 1143  
 Price, P. A. & McNaught, R. 2005, *GCN Circ.* No. 3164  
 Rykoff, E. S., et al. Feb. 2004, *ApJ*, 601, 1013  
 Sakamoto, T., et al. 2005, *GCN Circ.* No. 3173  
 Sari, R. & Esin, A. A. Feb. 2001, *ApJ*, 548, 787  
 Stetson, P. B. Mar. 1987, *PASP*, 99, 191  
 Vestrand, W. T., et al. May 2005, *Nature*, 435, 178